



Contents lists available at ScienceDirect

Biochemical and Biophysical Research Communications

journal homepage: www.elsevier.com/locate/ybbrc



Pba3–Pba4 heterodimer acts as a molecular matchmaker in proteasome α -ring formation



Kenji Takagi^{a,1}, Yasushi Saeki^b, Hideki Yashiroda^c, Hirokazu Yagi^a, Ai Kaiho^b, Shigeo Murata^c, Takashi Yamane^d, Keiji Tanaka^b, Tsunehiro Mizushima^{a,1,*}, Koichi Kato^{a,e,*}

^a Graduate School of Pharmaceutical Sciences, Nagoya City University, 3-1 Tanabe-dori, Mizuho-ku, Nagoya 467-8603, Japan

^b Laboratory of Protein Metabolism, Tokyo Metropolitan Institute of Medical Science, 2-1-6 Kamikitazawa, Setagaya-ku, Tokyo 156-8506, Japan

^c Laboratory of Protein Metabolism, Department of Integrated Biology, Graduate School of Pharmaceutical Sciences, The University of Tokyo, Tokyo 113-0033, Japan

^d Department of Biotechnology, Graduate School of Engineering, Nagoya University, Chikusa-ku, Nagoya 464-8603, Japan

^e Institute for Molecular Science and Okazaki Institute for Integrative Bioscience, National Institutes of Natural Sciences, 5-1 Higashiyama Myodaiji, Okazaki 444-8787, Japan

ARTICLE INFO

Article history:

Received 21 June 2014

Available online 1 July 2014

Keywords:

Assembly chaperone

Molecular matchmaker

Proteasome

Structure-guided mutagenesis

ABSTRACT

Eukaryotic proteasome assembly is assisted by multiple dedicated chaperones. In yeast, formation of the heteroheptameric ring composed of α 1– α 7 subunits is promoted by the heterodimeric chaperone Pba3–Pba4. Here we reveal that in the absence of this dimeric chaperone, α 2 replaces α 4 during α -ring assembly, thereby giving rise to a non-productive complex that lacks α 4, β 1, β 5, β 6, and β 7 subunits and aggregates of α 4. Furthermore, our structure-guided mutational data demonstrate that the Pba3–Pba4 heterodimer acts as molecular matchmaker reinforcing the interaction between α 4 and α 5, which is the crucial step in the α -ring formation.

© 2014 Elsevier Inc. All rights reserved.

1. Introduction

Ubiquitin/proteasome-mediated proteolysis plays a regulatory role in a number of diverse cellular processes, including cell-cycle progression, DNA repair, apoptosis, immune response, signal transduction, transcription, metabolism, and protein quality control. The 26S proteasome, which is responsible for the degradation of ubiquitinated substrates, is a highly conserved proteolytic machine consisting of a proteolytically active 20S core particle (CP) and one or two 19S regulatory particles [1–3]. In eukaryotic cells, the 20S CP is composed of 28 subunits arranged in a twofold symmetric cylindrical shape of four stacked heteroheptameric rings. Each outer ring is composed of seven different but homologous α subunits, i.e., α 1– α 7, whereas each inner ring is constructed from seven different but homologous β subunits, i.e., β 1– β 7. These subunits are located at specific positions in the quaternary structure of

the 20S CP. Assembly of the eukaryotic 20S CP begins with α -ring formation; subsequently, β subunits are recruited at a specific position on the α -ring in the following order: β 2, β 3, β 4, β 5, β 6, β 1, and β 7 [4]. The C-terminal 15 residues of β 7 subunit bind to the cleft formed between β 1 and β 2 subunits in a *trans* manner, thereby promoting the formation of the 20S CP [5]. Completion of 20S CP assembly is accompanied by autocatalytic removal of the propeptides, unsealing the catalytic sites of the β subunits.

Accumulating evidence indicates that assembly of the proteasomal subunits is not a spontaneous process, but is assisted by a series of specific chaperones. It has been shown that human UMP1 and PAC1-4 and yeast Ump1 and Pba1–4 (Pba1/Poc1, Pba2/Poc2, Pba3/Poc3/Dmp2, and Pba4/Poc4/Dmp1) serve as assembly chaperones contributing to the formation of the 20S CP [6–8]. While Pba1 and Pba2 form a heterodimer and bind the α -ring of the 20S CP through their C-terminal HbYX motifs [9,10], a heterodimeric complex formed between Pba3 and Pba4 interacts with the α 5 subunit [9,11]. In contrast, Ump1 has been shown to be an intrinsically unstructured protein that forms a complex with assembly intermediates containing β subunit(s) and remains associated with the preholo-20S proteasome [12,13]. Elimination of these assembly chaperones results in malformation of the proteasome. For example, a complex smaller than 20S CP has been identified in *Apba3* and *Apba4* cells [11]. This complex contains the β 2 subunit and all α subunits, except for α 4. This abnormal

* Corresponding authors. Address: Picobiology Institute, Department of Life Science, University of Hyogo, 3-2-1 Kouto, Kamigori, Akoh, Hyogo 678-1297, Japan. Fax: +81 791 58 0215 (T. Mizushima). Address: Institute for Molecular Science and Okazaki Institute for Integrative Bioscience, National Institutes of Natural Sciences, 5-1 Higashiyama Myodaiji, Okazaki 444-8787, Japan. Fax: +81 564 59 5224 (K. Kato).

E-mail addresses: mizushi@sci.u-hyogo.ac.jp (T. Mizushima), kkatonmr@ims.ac.jp (K. Kato).

¹ Present address: Picobiology Institute, Department of Life Science, University of Hyogo, 3-2-1 Kouto, Kamigori, Akoh, Hyogo 678-1297, Japan.

complex was induced by the shut off of *PBA4* (or *PBA3*) expression but did not diminish promptly even when *PBA4* (or *PBA3*) expression resumed after complex formation. This suggested that the complex was not a normal on-pathway intermediate.

Despite the progress in structural studies, the mechanism by which assembly chaperones assist in the correct arrangement of the proteasome subunits is not well understood. Herein we address this issue by focusing on the functional mechanisms of the Pba3–Pba4 heterodimer.

2. Materials and methods

2.1. Strains and genetic manipulations

The *Escherichia coli* strain DH5 α was used for propagating plasmids. BL21 (DE3) cells were used for expression and purification of recombinant proteins. The methods used for manipulation of yeast have been described previously [14]. The following strains of *Saccharomyces cerevisiae* were used: YYS1297 (*MATa Δ lys2::TRP1 pre5::PRE5-3xFLAG-LEU2*); YYS1299 (*MATa Δ lys2::TRP1 pre5::PRE5-3xFLAG-LEU2: Δ pba4*); YT478 (*MATa his Δ 1 leu2 Δ 0 met15 Δ 0 ura3 Δ 0 PRE6-EGFP-kanMX4 Δ pba4::HIS3MX6*); YT480 (*MATa his Δ 1 leu2 Δ 0 met15 Δ 0 ura3 Δ 0 PRE6-EGFP-kanMX4*); and YT931 (*MATa his Δ 1 leu2 Δ 0 met15 Δ 0 ura3 Δ 0 PRE10-EGFP-kanMX4:: Δ pba4::HIS3MX6*).

2.2. Microscopic analysis

Cells harboring GFP-fused proteins were photographed using a Leica DM4000B microscope equipped with a HCX PL FLUOTAR 100 \times /1.30 objective (Leica) and a Leica DFC300 FX camera. Images were obtained and processed using LAS AF6000 software (Leica) and processed using Adobe Photoshop CS4.

2.3. MS analysis

Affinity purification of the proteasome and MS analysis were performed as described previously [14]. To quantify each CP subunit contained in the complex, we performed quantitative MS using stable isotope labeling in culture (SILAC); the WT background strains were grown in SILAC medium supplemented with “light” lysine, 12 C-Lys. To prepare the 20S CP that contained all the subunits stoichiometrically, we cultured the *PRE5-3xFLAG* cells, in which the CP α 6 subunit was tagged with 3xFLAG tag, in SILAC medium. The cells were lysed using glass beads in 50 mM Tris–HCl buffer (pH7.5) containing 100 mM NaCl, 10% glycerol, and Complete Protease Inhibitors (-EDTA, Roche). Then, the FLAG-tagged protein was recovered by adsorption to an antiFLAG M2 agarose (Sigma), followed by elution with 3xFLAG peptide in 50 mM Tris–HCl buffer (pH 7.5) containing 100 mM NaCl and 10% glycerol. Purified α 6-containing complexes were then separated by BN-PAGE using a NativePAGE™ Novex® 3–12% Bis–Tris Protein Gel (Life Technologies). The specific bands corresponding to the 20S CP were extracted. The same experimental steps were repeated for purification of isotope-labeled abnormal complex using a SILAC medium supplemented with “heavy” lysine, 13 C-Lys.

For quantitative MS analysis, the protein bands were excised, denatured with 0.5% RapiGest (Waters) in 50 mM Tris–HCl (pH 8.8), and digested with 20 ng/ml lysyl endopeptidase (Wako) for 16 h at 37 °C. The resulting peptides were combined and subjected to LC-MALDI TOF/TOF (AB SCIEX, 4800 MALDI TOF/TOF analyzer). MS and MS/MS data were processed using ProteinPilot software with Paragon Algorithm (AB SCIEX).

2.4. Protein expression and purification

Pba3, Pba4, and Pba4 mutants were expressed as described previously [11]. Proteasome subunits α 2, α 4, and α 5 were expressed from the pGEX4T plasmid (GE Healthcare) as GST fusion proteins. GST- α 2, GST- α 4, and GST- α 5 were purified using glutathione Sepharose 4B affinity chromatography. The GST moiety was cleaved from the α 5 by thrombin treatment. The protein was further purified using anion exchange chromatography on a HiTrap Q HP column (GE Healthcare) and gel filtration chromatography on a Superdex 75 column (GE Healthcare).

2.5. Pull-down assay

GST- α 4 and its mutant forms immobilized on glutathione-Sepharose resin were washed extensively with 20 mM Tris–HCl, pH 7.5 containing 150 mM NaCl. The Sepharose resins containing approximately 10 μ g of GST fusion proteins were incubated with 1 ml of the buffer containing 150 μ g of Pba3, 130 μ g of Pba4, and 220 μ g of α 5 for 1 h at 4 °C, and then washed three times with 1 ml of the buffer. Proteins bound to the glutathione-Sepharose resin were subjected to SDS–PAGE followed by CBB staining. Formation of protein complex was also confirmed by size-exclusion chromatography using a Superdex 200 10/300 column (GE Healthcare) equilibrated with 20 mM Tris–HCl, pH 7.5, containing 150 mM NaCl and 10 mM 2-mercaptoethanol, followed by SDS–PAGE and Western blotting against α 4.

2.6. Structural modeling

3D structural model of the proteasome α -ring interacting with Pba3–Pba4 was built on the basis of crystal structures of yeast 20S proteasome (PDB ID code 1RYP) [15] and the α 5 subunit complexed with the heterodimer of Pba3 and Pba4 Δ loop (PDB ID code 2Z5C) [11], by superimposing the C α atoms of the α 5 subunit using LSQKAB program from CCP4 suite [16,17]. The model was subjected to energy minimization process using CNS [18].

3. Results and discussions

3.1. The composition of abnormal complex in Δ pba4 cells

To define the functional role of the Pba3–Pba4 heterodimer precisely, we first characterized the abnormal complex observed in Δ pba4 cells. The α 6-containing complexes were purified and then separated using BN-PAGE (Fig. 1A). The specific bands for the 13 C-Lys-labeled abnormal complexes and unlabeled 20S CP were excised and digested into peptides. The resultant peptides were jointly subjected to LC–MS/MS analysis to quantify subunit composition. Although our previous western blot analysis identified the β 2 subunit and all the α subunits (except for α 4) in the abnormal complex [11], the quantitative composition has not been determined. The quantitative MS data presented here revealed that the subunit ratios of this abnormal complex were stoichiometric for α 1, α 3, α 5, α 6, α 7, β 2, β 3, and β 4. Intriguingly, the ratio of the α 2 subunit in this complex was twice as high in a normal complex (Fig. 1B, Supplementary Fig. 1), suggesting that the α 4 subunit was replaced by α 2.

We have previously reported that, among the α subunits, α 5 binds to Pba3–Pba4 most strongly [11]. This raises a possibility that Pba3–Pba4 controls the proper interaction between α 4 and α 5 during the α -ring formation. To test this possibility, we examined interactions of α 5 with α 2 and α 4 *in vitro* in the presence and absence of Pba3–Pba4 (Fig. 1C). We found that the interaction between α 4 and α 5 depends on Pba3–Pba4, while α 2 binds α 5

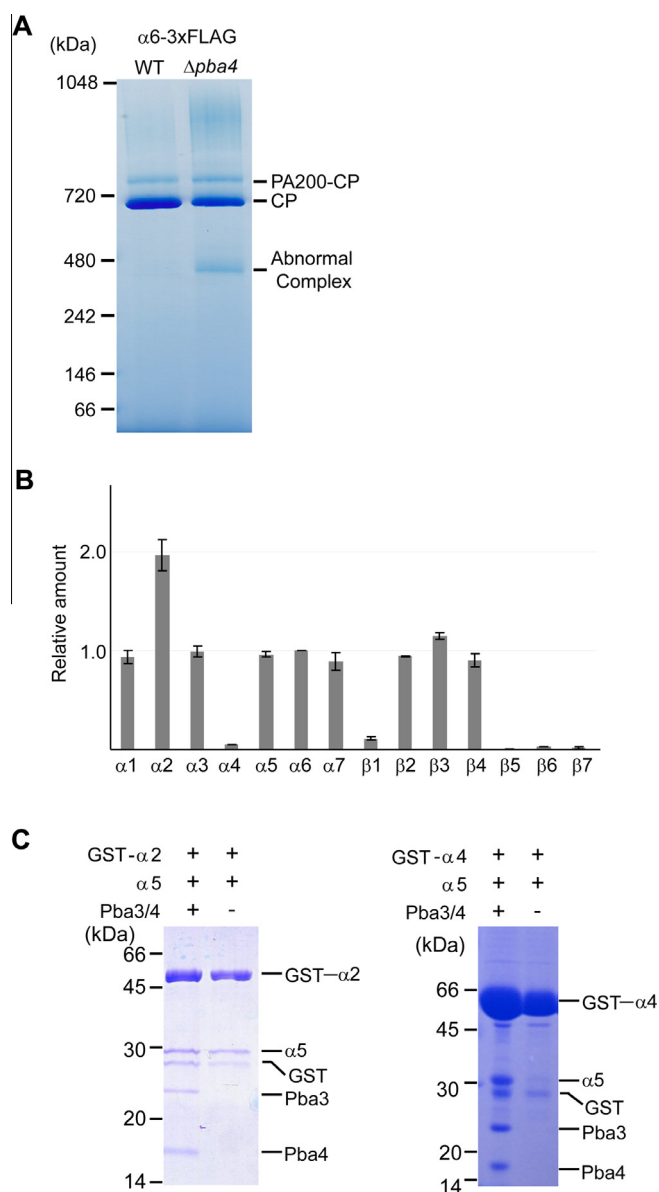


Fig. 1. Characterization of impaired α -ring formation in $\Delta pba4$ cells (A) Blue native (BN)-PAGE analysis of the $\alpha 6$ -containing complex in $\Delta pba4$ cells. Crude lysate from PRE5($\alpha 6$)-3xFLAG (YYS1297) and PRE5($\alpha 6$)-3xFLAG/ $\Delta pba4$ (YYS1299) strains were affinity-purified using AntiFLAG M2 beads and resolved using 3–12% BN-PAGE followed by CBB staining. Major protein bands were assigned to PA200/Blm10-CP, CP, and the abnormal complex (by LC-MS/MS analysis). (B) Quantitative MS analysis of subunit composition of the abnormal complex in $\Delta pba4$ cells. The amount of each subunit is shown in a bar graph, relative to the amount of $\alpha 6$ subunit. Values are mean \pm S.D., $n = 4$. (C) Protein-protein pull-down assay of interaction of $\alpha 5$ with GST- $\alpha 4$ or GST- $\alpha 2$ immobilized on glutathione-Sepharose gel in the presence or absence of Pba3–Pba4.

directly in a chaperone-independent manner. The formation of Pba3/4- $\alpha 5$ - $\alpha 4$ ternary complex was confirmed by size-exclusion chromatography (Supplementary Fig. 2). These data strongly suggest that the process of joining $\alpha 4$ and $\alpha 5$ is the hardest part of the α -ring formation, and $\alpha 2$ replaces $\alpha 4$ in the absence of the Pba3–Pba4 heterodimer.

3.2. Suppression of $\alpha 4$ aggregation by Pba3–Pba4

We next examined subcellular localization of the dislocated $\alpha 4$ subunit in the $\Delta pba4$ cells (Fig. 2). The $\alpha 4$ -GFP fusion protein was primarily localized in the nuclei of both $\Delta pba4$ and wild type cells

grown at 37 °C for 3 h, although the signal intensity of the GFP tag was slightly weakened in the absence of Pba4. Strikingly, in $\Delta pba4$ cells, $\alpha 4$ -GFP aggregated in the cytoplasm showing as a large dot-like structure. Such dots were not observed for $\alpha 7$ -GFP. Aggregates of $\alpha 4$ -GFP in $\Delta pba4$ cells were not observed at 27 °C, suggesting that the high temperature promoted the aggregation of $\alpha 4$ -GFP.

These data suggest that the deletion of *pba3* and *pba4* results in the formation of the non-productive complex containing an abnormal α -ring, in which a $\alpha 2$ subunit is embedded instead of $\alpha 4$, leaving the dislocated $\alpha 4$ subunits to accumulate as aggregates. Thus, the Pba3–Pba4 heterodimer contributes to suppression of intracellular accumulation of the $\alpha 4$ aggregates.

3.3. $\alpha 4$ – $\alpha 5$ matchmaking by Pba3–Pba4

To gain an insight into the mechanisms underlying the chaperone-dependent interaction between $\alpha 4$ and $\alpha 5$, we generated a 3D model of Pba3–Pba4 interactions with the α -ring based on superimposing the crystal structure of the $\alpha 5$ subunit to form complexed with Pba3–Pba4 Δ loop and the 20S CP (Fig. 3A). In the refined model, we found that Pba3–Pba4 interacts not only with $\alpha 5$ but also with $\alpha 4$ and $\alpha 6$ subunits. In particular, $\alpha 4$ makes contact exclusively with Pba4; Ser78, Lys89, Asp91, Asp95, His99, and Leu132 of Pba4 and Asp5, Ser95, Thr99, Leu100, Arg119, and Tyr120 of $\alpha 4$ form a binding interface. In this interface, Lys89 and His99 of Pba4 play central roles by multiple hydrogen bond formation and van der Waals interaction with $\alpha 4$, and the complementary charge interactions are mediated between Asp91 of Pba4 and Arg119 of $\alpha 4$ (Fig. 3B). Alanine substitutions of these amino acid residues resulted in significantly impaired interaction of GST-fused $\alpha 4$ with Pba3–Pba4 and $\alpha 5$ (Fig. 3C). These results suggest that the direct interaction between Pba4 and $\alpha 4$ is a prerequisite for its proper recruitment adjacent to $\alpha 5$.

3.4. Proteasome assembly assisted by Pba3–Pba4

We unexpectedly found that $\alpha 5$ has an intrinsically higher affinity for $\alpha 2$ than for $\alpha 4$, the inherent neighbor in the native α -ring. Our findings indicated that the Pba3–Pba4 heterodimer not

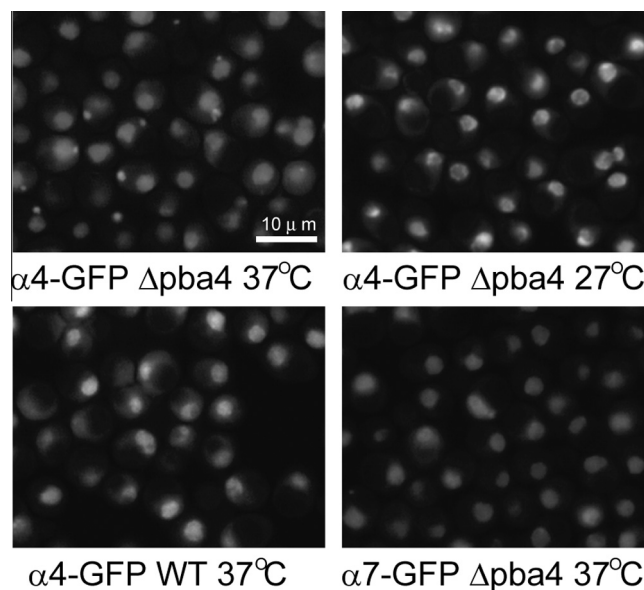


Fig. 2. Suppression of $\alpha 4$ aggregation by Pba3–Pba4 $\alpha 4$ -GFP aggregates in the cytoplasm of $\Delta pba4$ cells at high temperature. Cells expressing $\alpha 4$ -GFP or $\alpha 7$ -GFP were grown in YPD medium at 27 °C or 37 °C for 3 h.

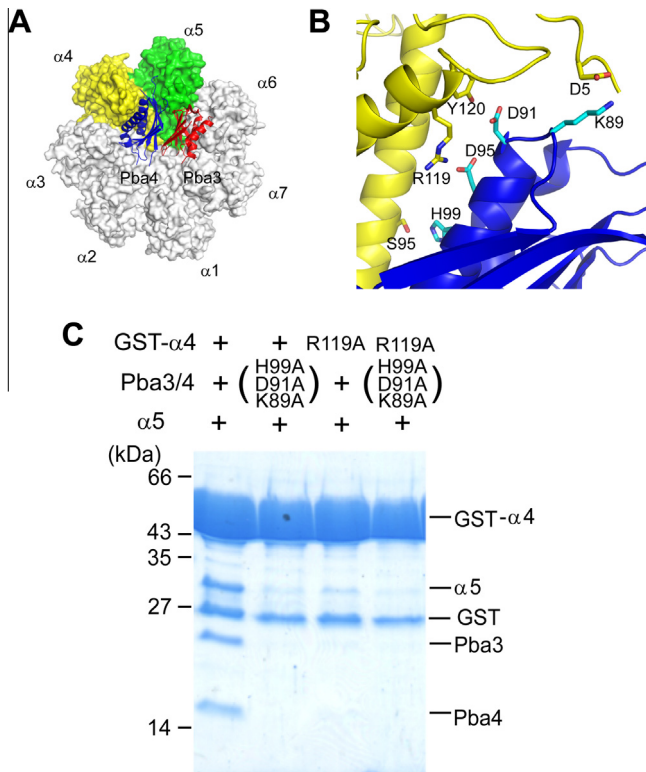


Fig. 3. Effects of the mutations of $\alpha 4$ and/or Pba4 on the Pba3–Pba4-dependent interaction (A) 3D model of the proteasome α -ring complexed with the Pba3–Pba4 heterodimer. Pba3 (red) and Pba4 (blue) are shown as a ribbon model, while the α subunits are shown as a surface model highlighting $\alpha 4$ (yellow) and $\alpha 5$ (green). (B) Close-up view of the interface between Pba4 and $\alpha 4$ is displayed in the right panel; residues involved in the interaction are shown in a stick representation. (C) Protein–protein pull-down assays of interaction of $\alpha 5$ with GST– $\alpha 4$ immobilized on glutathione–Sepharose gel in the presence of Pba3–Pba4 were performed for wild type and $\alpha 4$ -Pba4 binding-interface mutations.

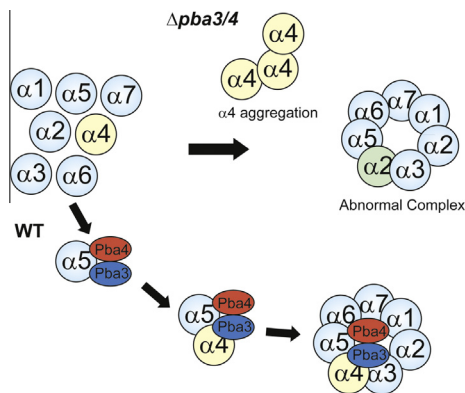


Fig. 4. Schematic model for the Pba3–Pba4-assisted α -ring formation. The Pba3–Pba4 heterodimer mediates the appropriate interaction between $\alpha 4$ and $\alpha 5$, facilitating the formation of α -ring and suppressing the aggregation of $\alpha 4$.

only captures $\alpha 5$ but also interacts with $\alpha 4$ through the charged residues of Pba4. On the basis of these data, we propose a mechanistic model in which Pba3–Pba4 acts as a molecular matchmaker that enhances the interaction between $\alpha 5$ and $\alpha 4$, thereby suppressing $\alpha 4$ aggregation, and contributes to the assembly of α -ring (Fig. 4).

Our structural inspection has suggested that the Pba3–Pba4 heterodimer is released from the assembly intermediate on

recruitment of the $\beta 4$ subunit in avoidance of steric clash [11]. Hence, it is conceivable that the subsequent subunit recruitments are achieved in the absence of this assembly chaperone complex and is primarily based on the complementary properties of the proteasomal subunits. In the intact 20S CP, the $\beta 5$ subunit is placed in contact with both $\alpha 4$ and $\alpha 5$ [15]. It is noteworthy that the $\alpha 4$ – $\beta 5$ interface is mediated by charge complementarities that are not conserved in $\alpha 2$. Thus, the misassembly of α -ring in the absence of Pba3 and/or Pba4 may result in the termination of β -ring formation, which is supported by our MS data. The proteasome assembly chaperones could become targets of novel anticancer drugs which antagonize functional proteasome formation [19]. Our findings also provide new clues for the design of inhibitors against proteasome biogenesis.

Conflict of interest

The authors declare no conflict of interest.

Acknowledgments

This work was supported by grants (24112008 to Y.S., 24657113 and 25102008 to K.K., 20051010 and 21025027 to T.M., and 10108871 to T.K.) from the Ministry of Education, Culture, Sports, Science and Technology (MEXT) of Japan, by the Targeted Proteins Research Program of MEXT (to T.M., K. Tanaka, and K.K.), and by the Okazaki ORION project. K. Takagi is a recipient of JSPS Research Fellowships for Young Scientists.

Appendix A. Supplementary data

Supplementary data associated with this article can be found, in the online version, at <http://dx.doi.org/10.1016/j.bbrc.2014.06.119>.

References

- [1] D. Finley, Recognition and processing of ubiquitin–protein conjugates by the proteasome, *Annu. Rev. Biochem.* 78 (2009) 477–513.
- [2] K. Tanaka, The proteasome: overview of structure and functions, *Proc. Jpn. Acad. Ser. B Phys. Biol. Sci.* 85 (2009) 12–36.
- [3] K. Tanaka, T. Mizushima, Y. Saeki, The proteasome: molecular machinery and pathophysiological roles, *Biol. Chem.* 393 (2012) 217–234.
- [4] Y. Hirano, T. Kaneko, K. Okamoto, M. Bai, H. Yashiroda, K. Furuyama, K. Kato, K. Tanaka, S. Murata, Dissecting beta-ring assembly pathway of the mammalian 20S proteasome, *EMBO J.* 27 (2008) 2204–2213.
- [5] A.J. Marques, C. Glanemann, P.C. Ramos, R.J. Dohmen, The C-terminal extension of the beta7 subunit and activator complexes stabilize nascent 20S proteasomes and promote their maturation, *J. Biol. Chem.* 282 (2007) 34869–34876.
- [6] S. Murata, H. Yashiroda, K. Tanaka, Molecular mechanisms of proteasome assembly, *Nat. Rev. Mol. Cell Biol.* 10 (2009) 104–115.
- [7] P.C. Ramos, R.J. Dohmen, PACemakers of proteasome core particle assembly, *Structure* 16 (2008) 1296–1304.
- [8] R. Rosenzweig, M.H. Glickman, Chaperone-driven proteasome assembly, *Biochem. Soc. Trans.* 36 (2008) 807–812.
- [9] A.R. Kusmierczyk, M.J. Kunjappu, R.Y. Kim, M. Hochstrasser, A conserved 20S proteasome assembly factor requires a C-terminal HbYX motif for proteasomal precursor binding, *Nat. Struct. Mol. Biol.* 18 (2008) 622–629.
- [10] B.M. Stadtmueller, E. Kish-Trier, K. Ferrell, C.N. Petersen, H. Robinson, D.G. Myszka, D.M. Eckert, T. Formosa, C.P. Hill, Structure of a proteasome Pba1–Pba2 complex: implications for proteasome assembly, activation, and biological function, *J. Biol. Chem.* 287 (2012) 37371–37382.
- [11] H. Yashiroda, T. Mizushima, K. Okamoto, T. Kameyama, H. Hayashi, T. Kishimoto, S. Niwa, M. Kasahara, E. Kurimoto, E. Sakata, K. Takagi, A. Suzuki, Y. Hirano, S. Murata, K. Kato, T. Yamane, K. Tanaka, Crystal structure of a chaperone complex that contributes to the assembly of yeast 20S proteasomes, *Nat. Struct. Mol. Biol.* 15 (2008) 228–236.
- [12] X. Li, A.R. Kusmierczyk, P. Wong, A. Emili, M. Hochstrasser, beta-Subunit appendages promote 20S proteasome assembly by overcoming an Ump1-dependent checkpoint, *EMBO J.* 26 (2007) 2339–2349.
- [13] Y. Uekusa, K. Okawa, M. Yagi-Utsumi, O. Serve, Y. Nakagawa, T. Mizushima, H. Yagi, Y. Saeki, K. Tanaka, K. Kato, Backbone H, C, and N assignments of yeast Ump1, an intrinsically disordered protein that functions as a proteasome assembly chaperone, *Biomol. NMR Assign.* (2013).

- [14] Y. Saeki, E.A. Toh, T. Kudo, H. Kawamura, K. Tanaka, Multiple proteasome-interacting proteins assist the assembly of the yeast 19S regulatory particle, *Cell* 137 (2009) 900–913.
- [15] M. Groll, L. Ditzel, J. Lowe, D. Stock, M. Bochtler, H.D. Bartunik, R. Huber, Structure of 20S proteasome from yeast at 2.4 Å resolution, *Nature* 386 (1997) 463–471.
- [16] CCP4, The CCP4 suite: programs for protein crystallography, *Acta Crystallogr. D Biol. Crystallogr.* 50 (1994) 760–763.
- [17] W. Kabsch, A solution for the best rotation to relate two sets of vectors, *Acta Crystallogr. A* 32 (1976) 922–923.
- [18] A.T. Brunger, P.D. Adams, G.M. Clore, W.L. DeLano, P. Gros, R.W. Grosse-Kunstleve, J.S. Jiang, J. Kuszewski, M. Nilges, N.S. Pannu, R.J. Read, L.M. Rice, T. Simonson, G.L. Warren, Crystallography & NMR system: a new software suite for macromolecular structure determination, *Acta Crystallogr. D Biol. Crystallogr.* 54 (1998) 905–921.
- [19] T. Doi, M. Yoshida, K. Ohsawa, K. Shin-ya, M. Takagi, Y. Uekusa, T. Yamaguchi, K. Kato, T. Hirokawa, T. Natsume, Total synthesis and characterization of thielocin B1 as a protein–protein interaction inhibitor of PAC3 homodimer, *Chem. Sci.* 5 (2014) 1860–1868.